

Possible Drug Candidates for Alzheimer's Disease Deduced from Studying their Binding Interactions with $\alpha 7$ Nicotinic Acetylcholine Receptor

Ruo-Xu Gu^{1,§}, Hui Gu^{1,§}, Zhi-Yuan Xie¹, Jing-Fang Wang², Hugo R. Arias³, Dong-Qing Wei^{1,4,*} and Kuo-Chen Chou^{1,4,#}

¹College of Life Science and Biotechnology, Shanghai Jiaotong University, Shanghai 200240, China;

²Bioinformatics Center, Key Lab of Systems Biology, Shanghai Institutes for Biological Sciences, Chinese Academy of Sciences, Shanghai 200031, China; ³Department of Pharmaceutical Sciences, College of Pharmacy, Midwestern University, Glendale, AZ 85308, USA; ⁴Gordon Life Science Institute, San Diego, CA 92130, USA



Abstract: Dysfunction in $\alpha 7$ nicotinic acetylcholine receptor (nAChR), a member of the Cys-loop ligand-gated ion channel superfamily, is responsible for attentional and cognitive deficits in Alzheimer's disease (AD). To provide useful information for finding drug candidates for the treatment of AD, a study was carried out according to the following procedures. (1) DMXBA, a partial agonist of the $\alpha 7$ nAChR, was used as a template molecule. (2) To reduce the number of compounds to be considered, the similarity search and flexible alignment were conducted to exclude those molecules which did not match the template. (3) The molecules thus obtained were docked to $\alpha 7$ nAChR. (4) To gain more structural information, the molecular dynamics (MD) simulations were carried out for 9 most favorable agonists obtained by the aforementioned docking studies. (5) By analyzing the hydrogen bond interaction and hydrophobic/hydrophilic interaction, the following seven compounds were singled out as possible drug candidates for AD therapy: gx-50, gx-51, gx-52, gx-180, open3d-99008, open3d-51265, open3d-60247.

Key Words: $\alpha 7$ nAChR, DMXBA, docking, MD simulation, chemical modification.

#Author Profile: Dr. Kuo-Chen Chou is the chief scientist of Gordon Life Science Institute. He is also an Advisory Professor of several Universities. Professor Chou has published over 350 papers in the fields of computer-aided drug design, bioinformatics, protein-structural prediction, low-frequency internal motion of protein and DNA and its biological functions, graphic rules in enzyme kinetics and other biological systems, and diffusion-controlled reactions of enzymes. For more information about Professor Kuo-Chen Chou, visit <http://gordonlifescience.org/members/kcchou/> or http://home.roadrunner.com/~kchou/kc_index.html, or <http://www.pami.sjtu.edu.cn/people/kcchou/>.

INTRODUCTION

Alzheimer's disease (AD) is the most common cause of senile dementia. The development of the disease is accompanied with the gradual spread of sticky plaques and clumps of tangled fibers that disrupt the delicate organization of nerve cells in the brain, undermining the normal communication among brain cells. Alzheimer's disease is a kind of protein structure disease; it is caused by incorrect folding of proteins [1-4]. Experiments showed that Taiho Pharmaceutical Company's new drug DMXBA, (3-[(2,4-dimethoxy)benzylidene]-anabaseine), a synthetic benzylidene derivative of anabaseine which was isolated from the nemertine worm *Amphiporus lactifloreus*, can improve the cognition condition and memory of the patients through selectively stimulating the $\alpha 7$ nAChR. The hydroxyl metabolites of DMXBA, which have been proved to be more effective at stimulating $\alpha 7$ nAChR *in vitro*, do not work as effective as DMXBA *in vivo* for their higher polarity that prevents them from enter-

ing the brain [5, 6]. Molecular modeling studies suggest that the volumes of DMXBA and its metabolites are somewhat larger than the size of $\alpha 7$ nAChR's active pocket [7, 8]. So it is anticipated that if these molecules by some modification could better fit the active pocket and enter the brain more quickly, they might stimulate the $\alpha 7$ nAChR, and thus, they might be more effectively used for the treatment of AD. The present study was initiated in an attempt to explore such a possibility.

METHODS AND THEORIES

For drug development, structural information of membrane protein channel is a key ingredient [9, 10]. Since it is very difficult to crystallize membrane proteins, NMR has become a powerful tool to determine the structures of membrane protein channels (see, e.g., [11-13]). Meanwhile, in order to timely acquire the desired information, many useful computational tools have been developed and utilized for drug design (see, e.g., [14-28]). In the current study, we approach the problem by using various structural bioinformatics tools [29, 30] as they were quite successful in providing useful insights for drug development in many areas [31-41].

*Address correspondence to this author at the College of Life Science and Biotechnology, Shanghai Jiaotong University, Shanghai 200240, China; Fax: +86-21-6136-9363; E-mail: lifescience@san.rr.com

§Equal contribution to this study

1. The First Screening: Similarity Search and Flexible Alignment

Similarity search and flexible alignment were conducted as the first screening to exclude the molecules which did not match the template DMXBA so as to reduce the number of compounds to be investigated in the next step. Two databases were used in the current study, namely the NCI (National Cancer Institute) database and the GX database; the latter is a small database including 227 structures that were distilled from traditional Chinese herb.

Before the similarity search, the fingerprints of all the compounds investigated were computed. The similarity overlap was set at 60%. Similar screening procedure was also used in finding inhibitors against severe acute respiratory syndrome (SARS) [42-45], human immunodeficiency virus (HIV) [46], and AD [47], as well as for finding effective antibacterial agents [48]. The screening procedure led our focus on nearly 590 compounds, of which, however, some molecules were too large in size in comparison with the template molecule and some were too strong in polarity, and hence were excluded for further consideration. The remaining molecules were then further screened by the Lipinski's "rule of 5" [18, 49], and only 100 qualified compounds (see Appendix A) were left to be further investigated by the flexible alignment.

Before the flexible alignment with DMXBA, the CHARMM22 force field [50] was used to compute the partial charges of the 100 qualified compounds. During the process of the flexible alignment, the energies of any two molecules to be aligned were subject to minimization. The single bond's revolving was permitted and the aromaticity, H-bond acceptor, H-bond donor as well as the volume of molecules were selected with the similarity terms. The alignment score, S , was automatically generated by the software used. Generally speaking, the lower the value of S , the more similar the two molecules concerned.

2. The Second Screening: Molecular Docking and Molecular Dynamics Simulation

Computational docking operation is a useful vehicle for investigating the interaction of a protein receptor with its ligand and revealing their binding mechanism as demonstrated by a series of studies [7, 29, 30, 35, 42-45, 51-59]. In the current study, the ligand concerned was first placed at the active pocket of the $\alpha 7$ nAChR whose atomic coordinates were taken from [37], and the docking program [60] was used to search for the most optimal conformation and orientation of the ligand by randomly generating a diversity set of conformations of the ligand [61]. The interaction energy, including the electrostatic interaction energy and vdW (van der Waals) interaction, were computed. In this study, the active binding site is represented as the cavity formed within the interface of two $\alpha 7$ units [37]. The flexible docking method was adopted; i.e., the receptor remains rigid while the ligand was flexible and was able to move freely within the active cavity during the entire docking process. When a new conformation was generated, the search for the favorable binding configuration was performed by the TABU search protocol [62, 63] in a 3D docking box. Such docking

operations were performed one-by-one for DMXBA as well as the 100 compounds obtained from the aforementioned screening procedure.

Those compounds with small size and most favorable docking results were selected for further MD (molecular dynamics) simulations. The MD study has made it possible to thoroughly search the conformational space and investigate the motion trajectory of the molecular interaction system under some specified thermodynamic conditions (e.g., constant temperature or constant pressure). The MD simulations were triggered by hydrogen bond breaking and making events of the ligand and receptor interactions, and the results thus obtained could provide further conformational searching information in space. The simulations were conducted under the NPT ensemble (300K and normal pressure) and lasted for 500 ps. The MD simulations performed by the in-house software called SAMM (Shanghai Molecular Modeling), and the parameters of CHARMM22 [50] force field were used for the flexible alignment, docking procedure and MD simulation.

3. Optimization and Modification of gx-50

The molecule gx-50 is one of the drug candidates obtained in the above first two steps. According to the docking and MD simulation results, it was observed that some molecules (such as gx-180, gx-51, and gx-52) in the GX database exhibited good affinity for the $\alpha 7$ nAChR, it is worthwhile to study gx-50 for more details.

In order to explore the structure-activity relationship and find better compounds, we conducted the modification of gx-50 by designing its homologues and bioisosters [64]. The molecules thus generated are shown in Fig. (1), where panel (A) is for its homologues (schemes 1-7) and panel (B) for its bioisosters (schemes 8-12). All these molecules were respectively docked at the interface of two $\alpha 7$ subunits in order to determine their affinity for the $\alpha 7$ nAChR.

RESULTS AND DISCUSSION

The interaction energies obtained by docking the template molecule DMXBA and the 100 qualified compounds to the $\alpha 7/\alpha 7$ subunit interface are also given in Appendix A, where the binding energy is $U_{\text{binding}} = U_{\text{ele}} + U_{\text{vdw}}$, i.e., the sum of the electrostatic interaction and the van der Waals interaction. From the 101 compounds listed in Appendix A, 21 compounds (including DMXBA) were singled out as having lower binding energy than the others (see Table 1).

Shown in Fig. (2) are the structure of the template molecule (panel A) and a close view of its interactions (panel B) with the residues around the active cavity of the receptor based on the MD simulation results. Generally speaking, the lower the binding energy, the better the ligand is matched with the receptor. Hence, a compound having a lower binding energy with the receptor than DMXBA may likely have better affinity with the receptor than DMXBA does.

It can be seen from Appendix A that there are 43 compounds that have lower binding energy for the $\alpha 7$ nAChR than DMXBA. However, whether a molecule has high

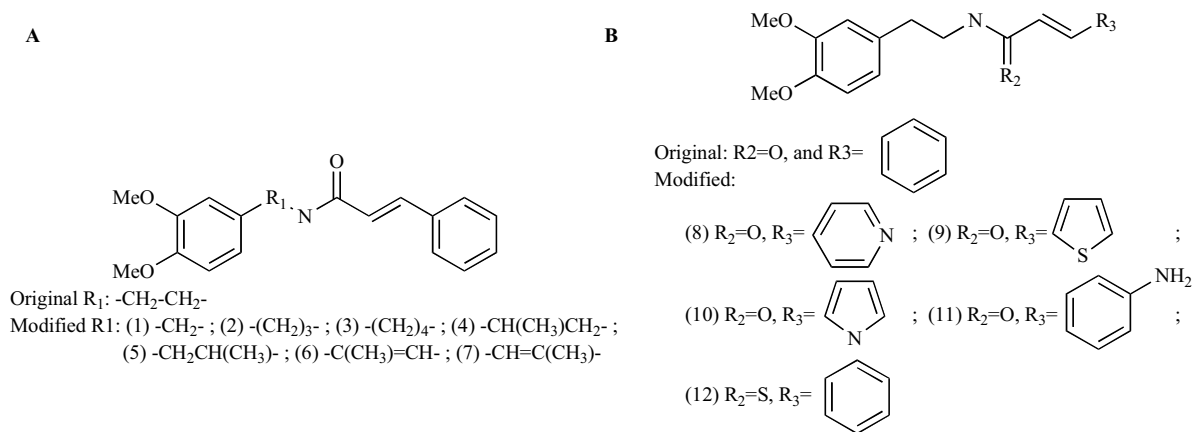


Fig. (1). The analogues we designed for (A) homologues and (B) bioisosters.

Table 1. Results ^a Obtained by Docking DMXBA and Part of the 100 Qualified Compounds (see the Text and Appendix A) to the $\alpha 7$ nAChR

Molecule Code	U _{total} (kcal/mol)	U _{ele} (kcal/mol)	U _{vdw} (kcal/mol)	U _{ligand} (kcal/mol)	U _{binding} (kcal/mol)	Numbers of H Bond
aido1698	44.68	-1.55	-20.49	66.72	-22.04	1
open3d-77464	47.36	-1.91	-16.09	65.36	-18.01	3
gx-50	72.03	3.06	-9.33	78.31	-6.28	3
cana-36993	82.91	1.63	-5.26	86.54	-3.63	1
gx-51	365.32	-1.44	4.34	362.42	2.90	2
open3d-41249	87.35	-0.70	7.72	80.33	7.02	1
gx-52	75.27	-0.71	9.97	66.02	9.25	4
133573	129.80	0.49	16.79	112.52	17.28	1
aido5682	104.66	-0.45	22.26	82.85	21.81	2
198860	87.38	3.79	18.06	65.53	21.86	1
aido5758	112.78	4.40	17.90	90.48	22.30	1
80835	137.42	-1.10	33.31	105.21	32.21	1
gx-180	86.87	-3.60	39.34	51.14	35.74	4
open3d-19047	133.22	-2.82	40.50	95.54	37.68	1
open3d-99008	179.72	1.36	61.34	117.02	62.70	3
open3d-99662	172.55	-3.74	82.13	94.16	78.39	1
aug00-2d-14717	205.76	-0.84	84.10	122.50	83.26	1
aido42661	228.06	1.39	97.44	129.22	98.83	1
open3d-51265	280.58	1.83	101.66	177.10	103.49	3
open3d-60247	651.67	1.13	111.14	539.40	112.27	2
DMXBA	222.64	0.49	120.35	101.80	120.84	2

^a U_{ele}, U_{vdw}, and U_{ligand} stands for the electrostatic interaction energy, van der Waals interaction energy, and ligand energy, respectively; U_{binding} is the sum of U_{ele} and U_{vdw}, while U_{total} the sum of U_{ele}, U_{vdw} and U_{ligand}.

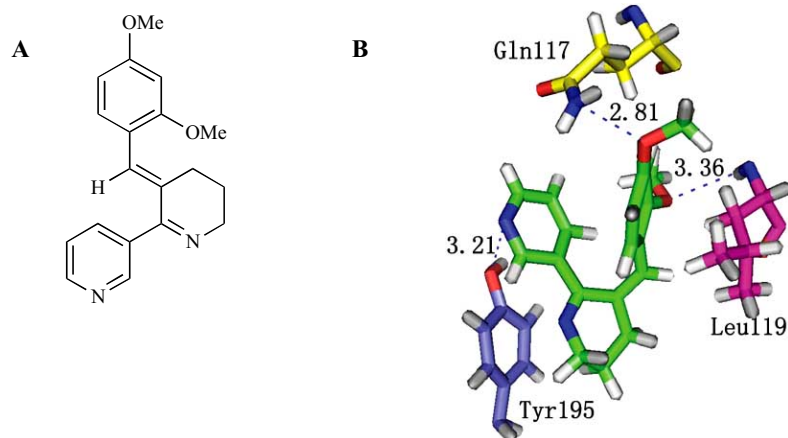


Fig. (2). Illustration to show (A) the template structure DMXBA, and (B) its detailed interactions with the residues around the active cavity of the receptor that were drawn based on the result of the MD simulation. The atoms in red, blue and grey stand for O, N and H, respectively. Specially, the carbon atoms in the ligand molecule are colored green. The hydrogen bonds are shown by blue dashed lines with unit of Å.

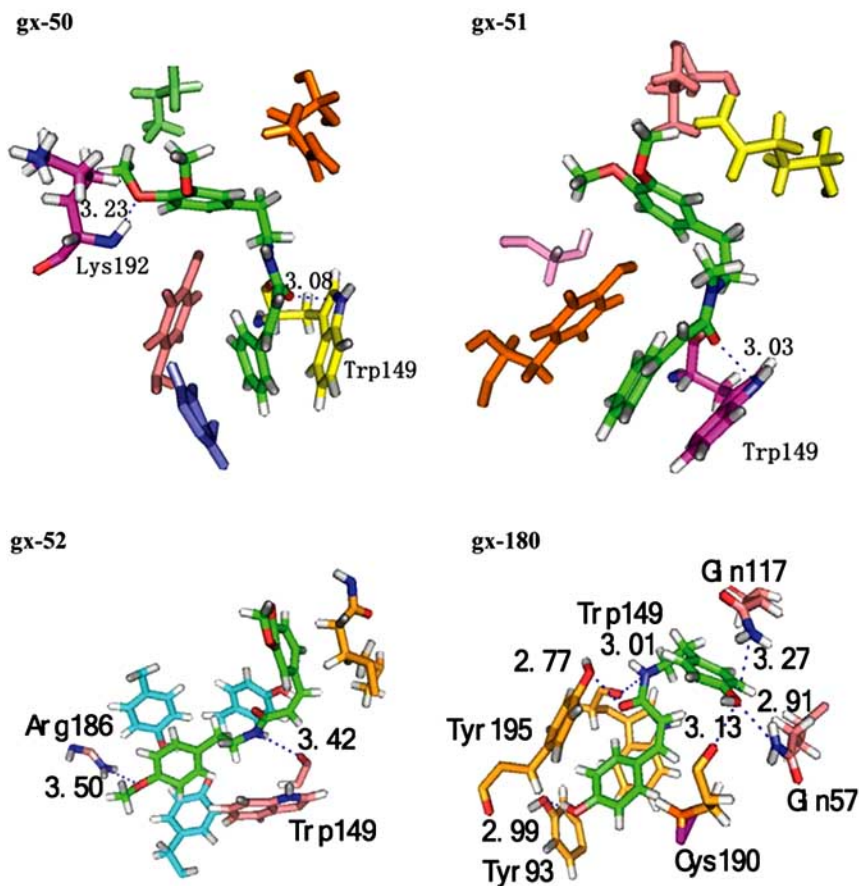


Fig. (3). A close view of the interactions of the four gx- series compounds singled out after the MD simulations with the residues around the active cavity of the receptor. See the legend of Fig. (2) for further explanation. The residues involved in forming the hydrogen bonds are labeled in the figure.

affinity with the receptor depends not only on the binding energy but also on the hydrogen bonding interactions [29, 35, 38, 65, 66] as well as on their hydrophobic/hydrophilic interaction [56, 67-69]. In other words, the binding energy alone should not be considered as the only criterion. By carefully analyzing all these interactions, we have found that,

although some compounds have quite low binding energies, their volumes are so small that they cannot fully occupy the active cavity of the receptor. This kind of molecules should be excluded as drug candidates. Also, as we can see from Appendix A, some compounds have no hydrogen bond formed with the receptor at all, e.g., 116378, aug-oct99-46,

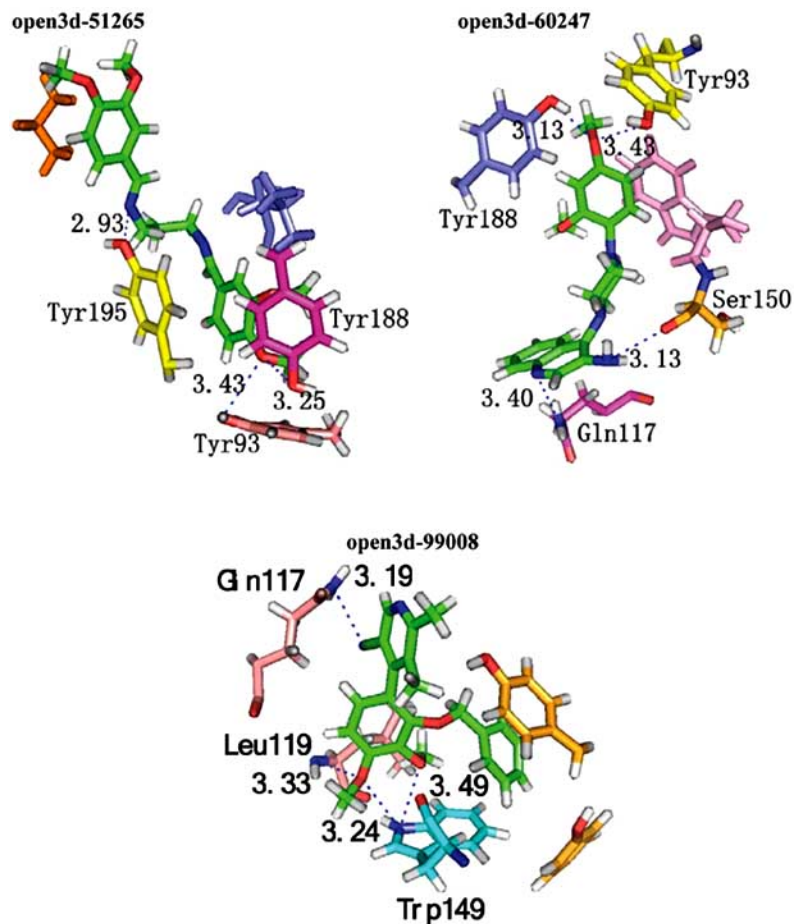
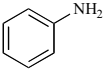
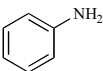


Fig. (4). A close view of the interactions of the three open3d- series molecules singled out after the MD simulations with the residues around the active cavity of the receptor. See the legend of Fig.2 for further explanation. The residues involved in forming the hydrogen bonds are labeled in the figure.

Table 2. The Interaction Energies and the Hydrogen Bonds Formed by Docking the 12 gx-50 Analogues of Fig.1 to the Receptor

No.	U_ele (kcal/mol)	U_vdw (kcal/mol)	U_binding (kcal/mol)	U_ligand (kcal/mol)	H Bond Length (Å)	H Bond Donor	H Bond Acceptor
1	0.07	-7.93	-7.86	78.83	2.94	Lys192	C=O
2	-0.88	18.17	17.29	87.73	2.54	-NH ₂	Gln117
3	-0.17	115.03	114.86	107.84	3.10	-NH ₂	Ser148
4	1.58	1.63	3.21	75.57	2.58	Lys192	-OCH ₃
					2.90	-NH ₂	Cys191
					3.85	Glu193	-OCH ₃
					3.04	Trp149	C=O
5	0.58	35.59	36.17	110.40	2.82	-NH ₂	Tyr188
6	-1.86	12.32	10.46	74.09	—	—	—
7	0.08	511.83	511.91	99.88	2.37	Leu119	-OCH ₃
8	-0.98	-13.50	-14.47	81.44	3.21	Gln57	-OCH ₃

(Table 2. Contd....)

No.	U _{ele} (kcal/mol)	U _{vdw} (kcal/mol)	U _{binding} (kcal/mol)	U _{ligand} (kcal/mol)	H Bond Length (Å)	H Bond Donor	H Bond Acceptor
9	3.54	23.57	27.11	130.15	3.04	Trp149	-OCH ₃
					2.93	Tyr195	-OCH ₃
10	1.07	-4.79	-3.73	67.44	—	—	—
11	-2.44	63.91	61.47	78.56	1.83	-NH ₂	Trp149
					1.67		Tyr188
					2.62		Tyr93
					3.01	Lys192	-OCH ₃
12	2.55	-14.77	-12.22	78.83	3.11	Leu119	C=S
					2.67	-NH ₂	Trp149

Appendix A. Results^a obtained by docking DMXBA and the 100 qualified compounds (see text) to the $\alpha 7$ nAChR. The first column is the molecule code (those beginning with 'gx' are the molecules from the GX database while others are from the NCI database). The result of DMXBA is shown in bold-face type.

Molecule Code	U _{total} (kcal/mol)	U _{ele} (kcal/mol)	U _{vdw} (kcal/mol)	U _{ligand} (kcal/mol)	U _{binding} (kcal/mol)	Numbers of Hydrogen Bond
aido1698	44.68	-1.55	-20.49	66.72	-22.04	1
cana-25948	39.65	2.70	-21.18	58.13	-18.48	0
open3d-77464	47.36	-1.91	-16.09	65.36	-18.01	3
aug00-2d-46041	44.90	0.88	-9.10	53.12	-8.22	0
gx-50	72.03	3.06	-9.33	78.31	-6.28	3
aug00-2d-52484	56.84	-1.42	-3.55	61.80	-4.96	0
cana-36993	82.91	1.63	-5.26	86.54	-3.63	1
aug00-2d-46946	61.67	2.20	-5.61	65.07	-3.40	0
cana-3563	57.95	1.95	-4.40	60.40	-2.44	0
116378	74.23	0.34	-1.51	75.40	-1.17	0
gx-51	365.32	-1.44	4.34	362.42	2.90	2
aug-oct99-46	90.63	1.44	5.14	84.05	6.58	0
211561	104.74	-0.48	7.43	97.79	6.95	0
open3d-41249	87.35	-0.70	7.72	80.33	7.02	1
gx-52	75.27	-0.71	9.97	66.02	9.25	4
diversity-1416	63.21	0.94	9.33	52.94	10.26	0
133573	129.80	0.49	16.79	112.52	17.28	1
aido5682	104.66	-0.45	22.26	82.85	21.81	2

(Appendix A. Contd....)

Molecule Code	U_{total} (kcal/mol)	U_{ele} (kcal/mol)	U_{vdw} (kcal/mol)	U_{ligand} (kcal/mol)	U_{binding} (kcal/mol)	Numbers of Hydrogen Bond
198860	87.38	3.79	18.06	65.53	21.86	1
aido5758	112.78	4.40	17.90	90.48	22.30	1
cana-21613	92.09	1.89	28.97	61.24	30.85	0
80835	137.42	-1.10	33.31	105.21	32.21	1
gx-180	86.87	-3.60	39.34	51.14	35.74	4
open3d-19047	133.22	-2.82	40.50	95.54	37.68	1
138360	161.50	-1.62	40.13	123.00	38.51	0
aug00-2d-197568	122.04	0.32	38.73	82.99	39.05	0
aido5683	121.09	1.38	41.22	78.49	42.60	0
aug00-2d-10419	139.85	2.46	40.86	96.53	43.32	0
aug00-2d-110397	200.67	5.40	38.74	156.53	44.14	0
aug00-2d-43675	102.83	-1.76	46.15	58.44	44.39	0
gx-138	66.75	11.31	37.97	17.48	49.28	0
open3d-83128	169.26	-0.07	52.89	116.44	52.82	0
cana-3412	152.19	1.94	53.58	96.67	55.52	0
open3d-99008	179.72	1.36	61.34	117.02	62.70	3
aug00-2d-21856	163.52	-0.58	72.30	91.80	71.72	0
aug00-2d-79612	277.49	-2.76	78.92	201.34	76.15	0
aug00-2d-194062	166.74	-0.13	76.41	90.46	76.28	0
open3d-99662	172.55	-3.74	82.13	94.16	78.39	1
aug00-2d-14717	205.76	-0.84	84.10	122.50	83.26	1
aido42661	228.06	1.39	97.44	129.22	98.83	1
open3d-51265	280.58	1.83	101.66	177.10	103.49	3
open3d-60247	651.67	1.13	111.14	539.40	112.27	2
134516	205.35	0.05	114.82	90.48	114.87	0
DMXBA	222.64	0.49	120.35	101.80	120.84	2
aido7132	232.88	-2.34	124.22	111.00	121.88	0
aug00-2d-194063	232.43	-1.06	125.33	108.16	124.27	0
aido6142	241.74	-0.29	124.76	117.27	124.47	0
aug00-2d-201507	213.80	0.65	126.13	87.02	126.78	0
open3d-69548	269.65	1.50	127.05	141.09	128.56	0
aug00-2d-100664	445.99	1.55	130.70	313.74	132.25	0
aido6142	217.33	-2.99	137.60	82.73	134.61	0
diversity-304	229.32	2.94	142.27	84.11	145.21	0

(Appendix A. Contd....)

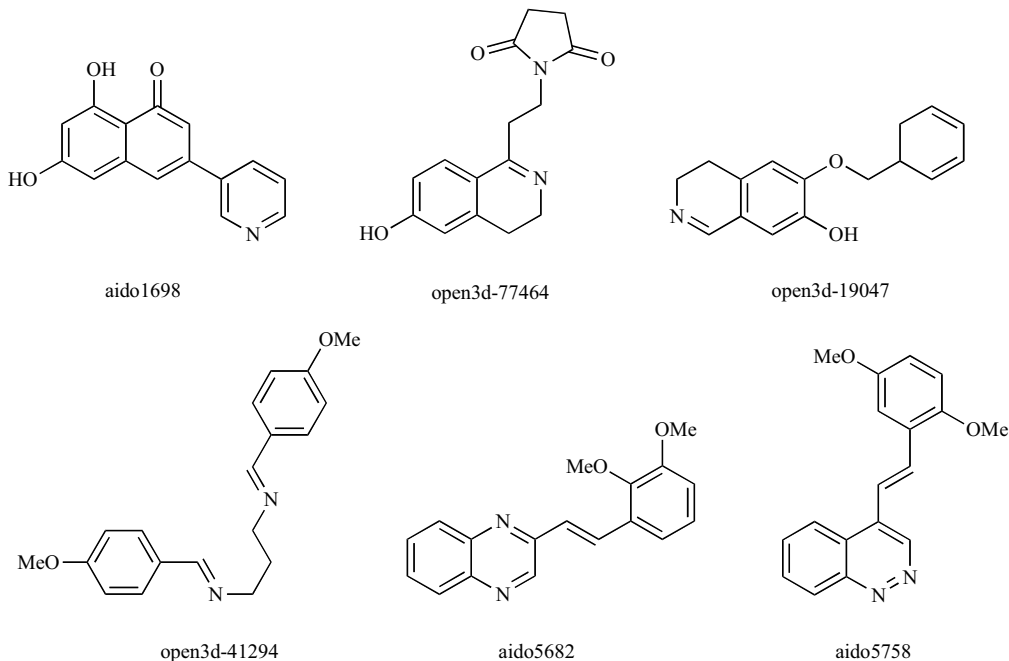
Molecule Code	U_{total} (kcal/mol)	U_{ele} (kcal/mol)	U_{vdw} (kcal/mol)	U_{ligand} (kcal/mol)	U_{binding} (kcal/mol)	Numbers of Hydrogen Bond
open3d-113735	247.64	0.13	145.42	102.09	145.56	0
aug00-2d-87177	238.84	-0.39	150.22	89.01	149.83	0
open3d-81530	274.36	2.66	147.67	124.02	150.34	0
open3d-36726	240.15	1.72	152.28	86.14	154.00	0
open3d-77465	302.00	-2.91	156.94	147.96	154.04	0
aug00-2d-83522	291.94	3.37	166.71	121.87	170.08	0
open3d-75607	334.77	2.73	171.30	160.74	174.03	0
open3d-99661	288.36	-0.23	182.51	106.08	182.27	0
aido21346	312.47	1.85	197.09	113.53	198.94	0
aug00-2d-99726	368.43	-3.75	203.66	168.53	199.91	0
aido5504	314.33	-0.87	217.76	97.45	216.89	0
aug00-2d-83534	406.88	1.60	226.00	179.28	227.60	0
open3d-25553	341.88	1.64	229.12	111.12	230.75	0
open3d-19958	369.42	-1.94	237.37	133.99	235.43	0
aug00-2d-154975	315.54	0.73	235.31	79.50	236.04	0
aug00-2d-67766	373.92	4.15	243.00	126.77	247.15	0
aido37806	356.42	-0.85	257.74	99.53	256.89	0
aug00-2d-211506	548.23	-0.67	281.80	267.10	281.14	0
aido9475	550.58	10.91	278.99	260.69	289.89	0
aug00-2d-87296	410.76	3.17	289.37	118.21	292.54	0
aug00-2d-114041	378.00	-2.71	295.33	85.39	292.61	0
open3d-42138	407.86	-1.84	306.71	102.98	304.87	0
93048	461.62	3.54	325.43	132.65	328.97	0
aug00-2d-100685	472.83	-0.27	330.00	143.09	329.74	0
aug00-2d-133964	451.92	1.89	329.51	120.52	331.40	0
aug00-2d-5788	436.24	2.65	331.55	102.05	334.19	0
cana-20059	527.82	-1.19	346.79	182.21	345.61	0
open3d-37127	463.46	-1.16	349.84	114.78	348.68	0
aido5579	453.42	-1.21	356.97	97.66	355.76	0
aug00-2d-249127	530.65	-1.02	434.62	97.05	433.60	0
open3d-116530	785.87	0.01	567.47	218.39	567.48	0
139117	855.32	0.67	575.83	278.83	576.49	0
aug00-2d-83502	1177.59	-0.20	587.00	590.79	586.80	0
aido15991	796.04	0.74	605.87	189.43	606.61	0

(Appendix A. Contd....)

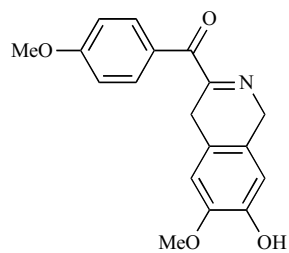
Molecule Code	U_{total} (kcal/mol)	U_{ele} (kcal/mol)	U_{vdw} (kcal/mol)	U_{ligand} (kcal/mol)	U_{binding} (kcal/mol)	Numbers of Hydrogen Bond
aug00-2d-61779	707.66	-0.58	624.44	83.80	623.86	0
open3d-75293	1167.85	0.52	757.84	409.50	758.36	0
aug00-2d-156466	1182.11	-0.87	867.93	315.04	867.07	0
aido42660	1044.55	-1.12	911.77	133.91	910.64	0
65578	1250.48	-1.16	1079.84	171.81	1078.68	0
aug00-2d-83536	1494.54	-1.14	1155.32	340.36	1154.18	0
aido14351	1372.75	1.46	1217.88	153.41	1219.34	0
aug00-2d-80642	1396.77	0.21	1256.28	140.28	1256.49	0
aido2936	2204.85	1.04	1275.30	928.51	1276.35	0
open3d-92327	1582.33	-1.11	1430.38	153.05	1429.28	0
aug00-2d-184056	1780.01	-2.33	1481.50	300.83	1479.17	0
aug00-2d-116383	2262.50	1.40	1619.33	641.78	1620.72	0
aido15987	1981.29	1.28	1673.08	306.94	1674.36	0
aug00-2d-249066	1988.48	0.67	1860.15	127.65	1860.83	0
aido6569	7264.30	1.96	5334.16	1928.17	5336.13	0

^a U_{ele} , U_{vdw} , and U_{ligand} stands for the electrostatic interaction energy, van der Waals interaction energy, and ligand energy, respectively; U_{binding} is the sum of U_{ele} and U_{vdw} , while U_{total} the sum of U_{ele} , U_{vdw} and U_{ligand} .

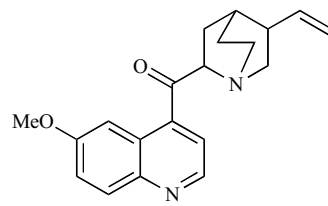
Appendix B. The structures of the 20 compounds with hydrogen bonds formed with the receptor after the docking operation.



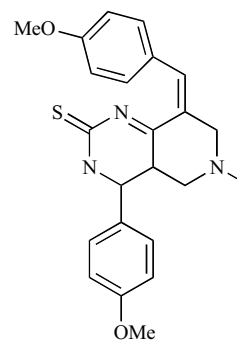
(Appendix B. Contd....)



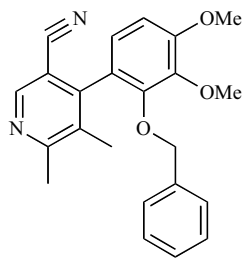
open3d-99662



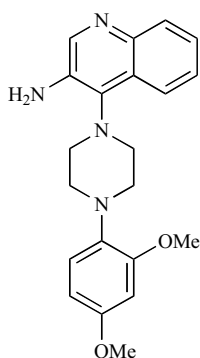
aug00-2d-14714



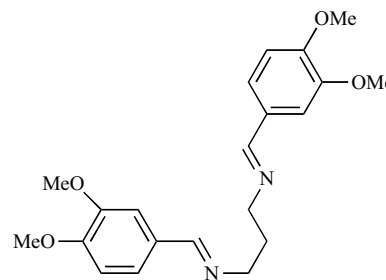
aido42661



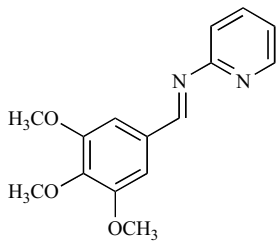
open3d-99008



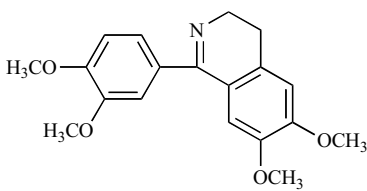
open3d-60247



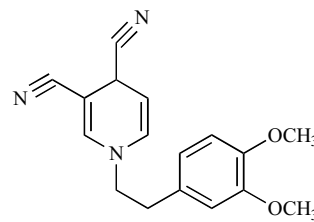
open3d-51265



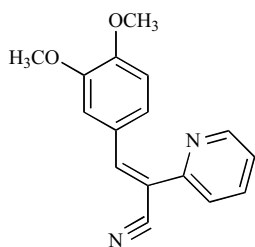
cana-36993



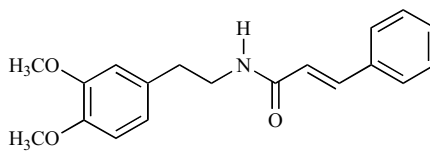
133573



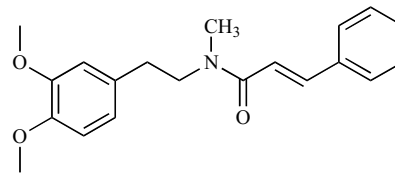
80835



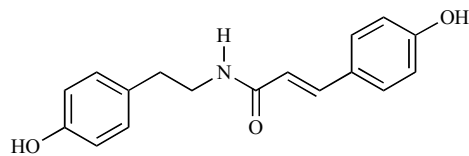
198860



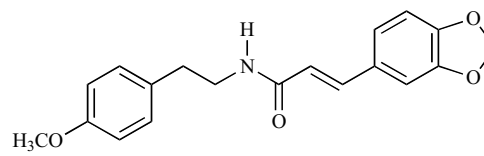
gx-50



gx-51



gx-180



gx-52

211561, aug00-2d-10419, aug00-2d-43675, etc. Those compounds with hydrogen bonds formed with the receptor are the following 20 compounds: aido1698, open3d-77464, gx-50, cana-36993, gx-51, open3d-41249, gx-52, 133573, aido5682, 198860, aido5758, 80835, gx-180, open3d-19047, open3d-99008, open3d-99662, aug00-2d-14717, aido42661, open3d-51265 and open3d-60247. The structures of these molecules are listed in Appendix B. Eleven of them formed only one hydrogen bond while the other nine formed two or more.

The nine molecules that have formed two or more hydrogen bonds with the $\alpha 7$ receptor are: open3d-77464, gx-50, gx-51, gx-52, aido5682, gx-180, open3d-99008, open3d-51265 and open3d-60247. Such nine molecules were further investigated by means of MD simulations. After the MD simulation, the corresponding hydrogen bond numbers became 0, 2, 1, 2, 0, 6, 4, 3, and 4, respectively. By removing those with hydrogen bond disappearing, we have the following seven compounds: gx-50, gx-51, gx-52, gx-180, open3d-99008, open3d-51265, open3d-60247. From the seven compounds, four belong to the gx-series and three to the open3d-series. A close view of the interactions for the four gx-series compounds with the residues around the active cavity of the receptor is given in Fig. (3), while that for the three open3d-series compounds is given in Fig. (4). In both figures, the residues involved in forming the hydrogen bonds are labeled.

As mentioned above, compounds 1-7 shown in Fig. (1A) are the homologues we designed. Their docking results are given in Table 2 with indexes 1-7, respectively. It is obviously that the methoxyl group plays a critical role as a hydrogen bond acceptor and the acidamide group is also important in forming hydrogen bond with the $\alpha 7$ receptor. The differences in the carbon chain (including the length of the carbon chain, either linear alkyl chains or branched alkyl chains or alkene chains) will affect the locations of both the acidamide and the methoxyl in the $\alpha 7$ receptor, and thus will affect the number of hydrogen bonds formed between the ligand and the $\alpha 7$ receptor. It will also affect the interaction energy, especially the van der Waals interaction energy through its volume and geometry shape.

Compounds 8-12 shown in Fig. (1B) are the bioisosters of gx-50. Their docking results are given in Table 2 with indexes 8-12, indicating that a suitable substituent in R₃ can also decrease the binding energy. However, the influence on the electrostatic interaction energy is not quite obvious as expected.

Table 2 shows that some of the analogues (e.g. Nos.4 and 11) have formed four hydrogen bonds with the receptor in contrast to three formed by gx-50 (see Table 1), meaning that they have even stronger hydrogen bond interaction than gx-50.

CONCLUSION

It is deduced through this study that the following seven compounds present high chances to become lead candidates for the development of AD therapy: gx-50, gx-51, gx-52, gx-180, open3d-99008, open3d-51265, open3d-60247 (Fig. 3 and Fig. 4). However, the molecule gx-180 may be of too strong polarity to infiltrate the meninges.

The docking results from the gx-50 analogues may provide useful clues for the structure-activity relationship investigation. Some of them may be worthwhile to be tested by experiments to further investigate their effects. In this regard, an important fact that needs to be considered is that although these compounds may bind to the $\alpha 7$ nAChR binding pocket with high affinity, they not necessarily will trigger receptor gating, a complex mechanism where ligand binding produces a conformational change in the extracellular portion of the receptor that is transmitted to the transmembrane domain, specifically moving the M2 transmembrane segments, which are the most important structural factors for ion channel activity [70]. In other words, we have to experimentally determine which compound activates the $\alpha 7$ nAChR and which compound behaves as a high-affinity competitive antagonist. The present study was focused on computational approaches, particularly from the angle of structural bioinformatics and molecular dynamics. The relevant experimental work is currently underway in collaboration with Prof. Zhongdong Qiao and Hugo Arias's laboratory. The results will be reported elsewhere.

ACKNOWLEDGEMENTS

This work was supported by the grants from the national 863 Bioinformatics Projects under the contract No. 2007AA02Z333, the national 973 program under the contract No. 2005CB724303 and the Chinese National Science Foundation under the Contract No.20773085 and 30870476, as well as the Major Chinese National Funding of New Drug Discovery for the Integrated Platform and the Virtual Laboratory for Computational Chemistry of CNIC, and the Supercomputing Center of CNIC, Chinese Academy of Sciences. This research was also partially supported by grants from the Science Foundation Arizona and Stardust Foundation and from the College of Pharmacy, Midwestern University (to HRA).

REFERENCES

- [1] Carter, D. B.; Chou, K. C. A model for structure dependent binding of Congo Red to Alzheimer beta-amyloid fibrils. *Neurobiol. Aging*, **1998**, *19*, 37-40.
- [2] Wang, J. F.; Wei, D. Q.; Lin, Y.; Wang, Y. H.; Du, H. L.; Li, Y. X.; Chou, K. C. Insights from modeling the 3D structure of NAD(P)H-dependent D-xylose reductase of *Pichia stipitis* and its binding interactions with NAD and NADP. *Biochem. Biophys. Res. Commun.*, **2007**, *359*, 323-329.
- [3] Kem, W. R. The brain alpha7 nicotinic receptor may be an important therapeutic target for the treatment of Alzheimer's disease: studies with DMXBA (GTS-21). *Behav. Brain Res.*, **2000**, *113*, 169-181.
- [4] Chou, K. C.; Howe, W. J. Prediction of the tertiary structure of the beta-secretase zymogen. *Biochem. Biophys. Res. Commun.*, **2002**, *292*, 702-708.
- [5] Meyer, E. M.; Tay, E. T.; Papke, R. L.; Meyers, C.; Huang, G. L.; de Fiebre, C. M. 3-[2,4-Dimethoxybenzylidene]anabaseine (DMXB) selectively activates rat alpha7 receptors and improves memory-related behaviors in a mecamylamine-sensitive manner. *Brain Res.*, **1997**, *768*, 49-56.
- [6] Kem, W. R.; Mahnir, V. M.; Prokai, L.; Papke, R. L.; Cao, X.; Le-Francois, S.; Wildeboer, K.; Prokai-Tatrai, K.; Porter-Papke, J.; Soti, F. Hydroxy metabolites of the Alzheimer's drug candidate 3-[(2,4-dimethoxy)benzylidene]-anabaseine dihydrochloride (GTS-21): their molecular properties, interactions with brain nicotinic receptors, and brain penetration. *Mol. Pharmacol.*, **2004**, *65*, 56-67.
- [7] Wei, D. Q.; Sirois, S.; Du, Q. S.; Arias, H. R.; Chou, K. C. Theoretical studies of Alzheimer's disease drug candidate [(2,4-dimethoxy) ben-

- zylidene]-anabaseine dihydrochloride (GTS-21) and its derivatives. *Biochem. Biophys. Res. Commun.*, **2005**, *338*, 1059-1064.
- [8] Kem, W.; Soti, F.; LeFrancois, S.; Wildeboer, K.; MacDougall, K.; Wei, D. Q.; Chou, K. C.; Arias, H. R. Review: The nemertine toxin anabaseine and its derivative DMXBA (GTS-21): chemical and pharmacological properties. *Marine Drugs*, **2006**, *4*, 255-273.
- [9] Miller, C. Ion channels: coughing up flu's proton channels. *Nature*, **2008**, *451*, 532-533.
- [10] Borman, S. Flu virus proton channel analyzed: Structures of key surface protein suggest different drug mechanisms. *Chem. Eng. News*, **2008**, *86*, 53-54.
- [11] Schnell, J. R.; Chou, J. J. Structure and mechanism of the M2 proton channel of influenza A virus. *Nature*, **2008**, *451*, 591-595.
- [12] Oxenoid, K.; Chou, J. J. The structure of phospholamban pentamer reveals a channel-like architecture in membranes. *Proc. Natl. Acad. Sci. U S A*, **2005**, *102*, 10870-10875.
- [13] Call, M. E.; Schnell, J. R.; Xu, C.; Lutz, R. A.; Chou, J. J.; Wucherpfennig, K. W. The structure of the zeta-zeta transmembrane dimer reveals features essential for its assembly with the T cell receptor. *Cell*, **2006**, *127*, 355-368.
- [14] Chou, K. C. A vectorized sequence-coupling model for predicting HIV protease cleavage sites in proteins. *J. Biol. Chem.*, **1993**, *268*, 16938-16948.
- [15] Chou, K. C. Review: Prediction of HIV protease cleavage sites in proteins. *Anal. Biochem.*, **1996**, *233*, 1-14.
- [16] Sirois, S.; Wei, D. Q.; Du, Q. S.; Chou, K. C. Virtual Screening for SARS-CoV Protease Based on KZ7088 Pharmacophore Points. *J. Chem. Inf. Comput. Sci.*, **2004**, *44*, 1111-1122.
- [17] Chou, K. C.; Shen, H. B. Signal-CF: a subsite-coupled and window-fusing approach for predicting signal peptides. *Biochem. Biophys. Res. Commun.*, **2007**, *357*, 633-640.
- [18] Sirois, S.; Hatzakis, G. E.; Wei, D. Q.; Du, Q. S.; Chou, K. C. Assessment of chemical libraries for their druggability. *Comput. Biol. Chem.*, **2005**, *29*, 55-67.
- [19] Chou, K. C.; Shen, H. B. MemType-2L: A web server for predicting membrane proteins and their types by incorporating evolution information through Pse-PSSM. *Biochem. Biophys. Res. Commun.*, **2007**, *360*, 339-345.
- [20] Sirois, S.; Tsoukas, C. M.; Chou, K. C.; Wei, D. Q.; Boucher, C.; Hatzakis, G. E. Selection of molecular descriptors with artificial intelligence for the understanding of HIV-1 protease peptidomimetic inhibitors-activity. *Med. Chem.*, **2005**, *1*, 173-184.
- [21] Shen, H. B.; Chou, K. C. Signal-3L: a 3-layer approach for predicting signal peptide. *Biochem. Biophys. Res. Commun.*, **2007**, *363*, 297-303.
- [22] Sirois, S.; Sing, T.; Chou, K. C. Review: HIV-1 gp120 V3 loop for structure-based drug design. *Curr. Protein Pept. Sci.*, **2005**, *6*, 413-422.
- [23] Shen, H. B.; Chou, K. C. EzyPred: A top-down approach for predicting enzyme functional classes and subclasses. *Biochem. Biophys. Res. Commun.*, **2007**, *364*, 53-59.
- [24] Sirois, S.; Touaibia, M.; Chou, K. C.; Roy, R. Glycosylation of HIV-1gp120 V3 loop: towards the rational design of a synthetic carbohydrate vaccine. *Curr. Med. Chem.*, **2007**, *14*, 3232-42.
- [25] Chou, K. C.; Shen, H. B. Review: Recent progresses in protein subcellular location prediction. *Anal. Biochem.*, **2007**, *370*, 1-16.
- [26] Emanuelsson, O.; Brunak, S.; von Heijne, G.; Nielsen, H. Locating proteins in the cell using TargetP, SignalP and related tools. *Nat. Protoc.*, **2007**, *2*, 953-971.
- [27] Chou, K. C.; Shen, H. B. Cell-PLoc: A package of web-servers for predicting subcellular localization of proteins in various organisms. *Nat. Protoc.*, **2008**, *3*, 153-162.
- [28] Chou, K. C.; Shen, H. B. HIVcleave: a web-server for predicting human immunodeficiency virus protease cleavage sites in proteins. *Anal. Biochem.*, **2008**, *375*, 388-390.
- [29] Chou, K. C. Structural bioinformatics and its impact to biomedical science. *Curr. Med. Chem.*, **2004**, *11*, 2105-2134.
- [30] Chou, K. C.; Wei, D. Q.; Du, Q. S.; Sirois, S.; Zhong, W. Z. Review: Progress in computational approach to drug development against SARS. *Curr. Med. Chem.*, **2006**, *13*, 3263-3270.
- [31] Althaus, I. W.; Chou, J. J.; Gonzales, A. J.; Diebel, M. R.; Chou, K. C.; Kezdy, F. J.; Romero, D. L.; Aristoff, P. A.; Tarpley, W. G.; Reusser, F. Steady-state kinetic studies with the non-nucleoside HIV-1 reverse transcriptase inhibitor U-87201E. *J. Biol. Chem.*, **1993**, *268*, 6119-6124.
- [32] Althaus, I. W.; Gonzales, A. J.; Chou, J. J.; Diebel, M. R.; Chou, K. C.; Kezdy, F. J.; Romero, D. L.; Aristoff, P. A.; Tarpley, W. G.; Reusser, F. The quinoline U-78036 is a potent inhibitor of HIV-1 reverse transcriptase. *J. Biol. Chem.*, **1993**, *268*, 14875-14880.
- [33] Althaus, I. W.; Chou, J. J.; Gonzales, A. J.; Diebel, M. R.; Chou, K. C.; Kezdy, F. J.; Romero, D. L.; Aristoff, P. A.; Tarpley, W. G.; Reusser, F. Kinetic studies with the nonnucleoside HIV-1 reverse transcriptase inhibitor U-88204E. *Biochem.*, **1993**, *32*, 6548-54.
- [34] Chou, K. C.; Kezdy, F. J.; Reusser, F. Review: Steady-state inhibition kinetics of processive nucleic acid polymerases and nucleases. *Anal. Biochem.*, **1994**, *221*, 217-230.
- [35] Chou, K. C.; Wei, D. Q.; Zhong, W. Z. Binding mechanism of coronavirus main proteinase with ligands and its implication to drug design against SARS. *Biochem. Biophys. Res. Commun.*, **2003**, *308*, 148-151. (Erratum: *ibid.*, **2003**, *310*, 675).
- [36] Chou, K. C. Modelling extracellular domains of GABA-A receptors: subtypes 1, 2, 3, and 5. *Biochem. Biophys. Res. Commun.*, **2004**, *316*, 636-642.
- [37] Chou, K. C. Insights from modelling the 3D structure of the extracellular domain of alpha7 nicotinic acetylcholine receptor. *Biochem. Biophys. Res. Commun.*, **2004**, *319*, 433-438.
- [38] Chou, K. C. Molecular therapeutic target for type-2 diabetes. *J. Proteome Res.*, **2004**, *3*, 1284-1288.
- [39] Chou, K. C. Modeling the tertiary structure of human cathepsin-E. *Biochem. Biophys. Res. Commun.*, **2005**, *331*, 56-60.
- [40] Chou, K. C. Insights from modeling the 3D structure of DNA-CBF3b complex. *J. Proteome Res.*, **2005**, *4*, 1657-1660.
- [41] Chou, K. C. Coupling interaction between thromboxane A2 receptor and alpha-13 subunit of guanine nucleotide-binding protein. *J. Proteome Res.*, **2005**, *4*, 1681-1686.
- [42] Wei, D. Q.; Zhang, R.; Du, Q. S.; Gao, W. N.; Li, Y.; Gao, H.; Wang, S. Q.; Zhang, X.; Li, A. X.; Sirois, S.; Chou, K. C. Anti-SARS drug screening by molecular docking. *Amino Acids*, **2006**, *31*, 73-80.
- [43] Wang, S. Q.; Du, Q. S.; Zhao, K.; Li, A. X.; Wei, D. Q.; Chou, K. C. Virtual screening for finding natural inhibitor against cathepsin-L for SARS therapy. *Amino Acids*, **2007**, *33*, 129-135.
- [44] Du, Q. S.; Wang, S. Q.; Jiang, Z. Q.; Gao, W. N.; Li, Y. D.; Wei, D. Q.; Chou, K. C. Application of bioinformatics in search for cleavable peptides of SARS-CoV Mpro and chemical modification of octapeptides. *Med. Chem.*, **2005**, *1*, 209-213.
- [45] Zhang, R.; Wei, D. Q.; Du, Q. S.; Chou, K. C. Molecular modeling studies of peptide drug candidates against SARS. *Med. Chem.*, **2006**, *2*, 309-314.
- [46] Gao, W. N.; Wei, D. Q.; Li, Y.; Gao, H.; Xu, W. R.; Li, A. X.; Chou, K. C. Agaritine and its derivatives are potential inhibitors against HIV proteases. *Med. Chem.*, **2007**, *3*, 221-226.
- [47] Zheng, H.; Wei, D. Q.; Zhang, R.; Wang, C.; Wei, H.; Chou, K. C. Screening for New Agonists against Alzheimer's Disease. *Med. Chem.*, **2007**, *3*, 488-493.
- [48] Li, Y.; Wei, D. Q.; Gao, W. N.; Gao, H.; Liu, B. N.; Huang, C. J.; Xu, W. R.; Liu, D. K.; Chen, H. F.; Chou, K. C. Computational approach to drug design for oxazolidinones as antibacterial agents. *Med. Chem.*, **2007**, *3*, 576-582.
- [49] Lipinski, C. A.; Lombardo, F.; Dominy, B. W.; Feeney, P. J. Experimental and computational approaches to estimate solubility and permeability in drug discovery and development settings. *Adv. Drug Deliv. Rev.*, **2001**, *46*, 3-26.
- [50] MacKerell Jr., A. D.; Bashford, D.; M. Bellott, M.; Dunbrack Jr., R. L.; Evanseck, J. D.; Field, M. J.; Fischer, S.; Gao, J.; Guo, H.; Ha, S.; Joseph-McCarthy, D.; Kuchnir, L.; Kuczera, K.; Lau, F. T. K.; Mattos, C.; Michnick, S.; Ngo, T.; Nguyen, D. T.; Prodhom, B.; Reiher, I., W. E.; Roux, B.; Schlenkerich, M.; Smith, J. C.; Stote, R.; Straub, J.; Watanabe, M.; Wiorkiewicz-Kuczera, J.; Yin, D.; Karplus, M. All-atom empirical potential for molecular modeling and dynamics studies of proteins. *J. Phys. Chem.*, **1998**, *102*, 3586-3616.
- [51] Du, Q. S.; Wang, S.; Wei, D. Q.; Sirois, S.; Chou, K. C. Molecular modeling and chemical modification for finding peptide inhibitor against SARS CoV Mpro. *Anal. Biochem.*, **2005**, *337*, 262-270.
- [52] Zhou, G. P.; Troy, F. A. 2nd NMR study of the preferred membrane orientation of polyisoprenols (dolichol) and the impact of their complex with polyisoprenyl recognition sequence peptides on membrane structure. *Glycobiol.*, **2005**, *15*, 347-359.
- [53] Zhou, G. P.; Troy, F. A. NMR studies on how the binding complex of polyisoprenol recognition sequence peptides and polyisoprenols can

- modulate membrane structure. *Curr. Protein Pept. Sci.*, **2005**, *6*, 399-411.
- [54] Wei, H.; Zhang, R.; Wang, C.; Zheng, H.; Chou, K. C.; Wei, D. Q. Molecular insights of SAH enzyme catalysis and their implication for inhibitor design. *J.Theor. Biol.*, **2007**, *244*, 692-702.
- [55] Li, L.; Wei, D. Q.; Wang, J. F.; Chou, K. C. Computational studies of the binding mechanism of calmodulin with chrysin. *Biochem. Biophys. Res. Commun.*, **2007**, *358*, 1102-1107.
- [56] Du, Q. S.; Wang, S. Q.; Chou, K. C. Analogue inhibitors by modifying oseltamivir based on the crystal neuraminidase structure for treating drug-resistant H5N1 virus. *Biochem. Biophys. Res. Commun.*, **2007**, *362*, 525-531.
- [57] Guo, X. L.; Li, L.; Wei, D. Q.; Zhu, Y. S.; Chou, K. C. Cleavage mechanism of the H5N1 hemagglutinin by trypsin and furin. *Amino Acids*, **2008**, *35*, 375-382.
- [58] Du, Q. S.; Sun, H.; Chou, K. C. Inhibitor design for SARS coronavirus main protease based on "distorted key theory". *Med. Chem.*, **2007**, *3*, 1-6.
- [59] Ye, Y.; Wei, J.; Dai, X.; Gao, Q. Computational studies of the binding modes of A_{2A} adenosine receptor antagonists. *Amino Acids*, **2008**, *35*, 389-396.
- [60] Morris, G. M.; Goodsell, D. S.; Halliday, R. S.; Huey, R.; Hart, W.E.; Belew, R. K.; Olson, A. J. Automated docking using a Lamarckian Genetic Algorithm and empirical binding free energy function. *J. Comput. Chem.*, **1998**, *19*, 1639-1662.
- [61] Kuntz, I. D.; Meng, E. C.; Shoichet, B. K. Structure-based strategies for drug design and discovery. *Acc. Chem. Res.*, **1994**, *27*, 117-123.
- [62] Glover, F. Tabu search: a tutorial. *Interfaces*, **1990**, *20*, 74-94.
- [63] Battiti, R.; Tecchiolli, G. Simulated annealing and tabu search in the long run: a comparison on qap tasks. *Comp. Math. Appl.*, **1994**, *28*, 1-8.
- [64] Wang, J. F.; Wei, D. Q.; Li, L.; Zheng, S. Y.; Li, Y. X.; Chou, K. C. 3D structure modeling of cytochrome P450 2C19 and its implication for personalized drug design. *Biochem. Biophys. Res. Commun.*, **2007**, *355*, 513-519. (Corrigendum: *ibid*, **2007**, *357*, 330).
- [65] Chou, K. C. Energy-optimized structure of antifreeze protein and its binding mechanism. *J. Mol. Biol.*, **1992**, *223*, 509-517.
- [66] Chou, K. C. Insights from modelling the tertiary structure of BACE2. *J. Proteome Res.*, **2004**, *3*, 1069-1072.
- [67] Connolly, M. L. Solvent-accessible surfaces of proteins and nucleic acids. *Science*, **1983**, *221*, 709-713.
- [68] Wang, S. Q.; Du, Q. S.; Chou, K. C. Study of drug resistance of chicken influenza A virus (H5N1) from homology-modeled 3D structures of neuraminidases. *Biochem. Biophys. Res. Commun.*, **2007**, *354*, 634-640.
- [69] Wei, D. Q.; Du, Q. S.; Sun, H.; Chou, K. C. Insights from modeling the 3D structure of H5N1 influenza virus neuraminidase and its binding interactions with ligands. *Biochem. Biophys. Res. Commun.*, **2006**, *344*, 1048-1055.
- [70] Lee, W. Y.; Sine, S. M. Principal pathway coupling agonist binding to channel gating in nicotinic receptors. *Nature*, **2005**, *438*, 243-247.